Contents lists available at ScienceDirect

International Journal of Refractory Metals and Hard Materials

journal homepage: www.elsevier.com

Sintering behavior and mechanical properties of spark plasma sintered β–SiAlON/TiN nanocomposites

Kh.A. Nekouee, R.A. Khosroshahi *

Faculty of Materials Engineering, Sahand University of Technology, Tabriz, Iran

ARTICLE INFO

Article history:
Received 24 February 2016
Received in revised form 29 July 2016
Accepted 3 August 2016
Available online xxx

Keywords:
β-SiAlON/TiN nanocomposites
Mechanical alloying
Spark plasma sintering
Mechanical properties

ABSTRACT

In this study, fully dense β-SiAlON/TiN composites were produced by Spark Plasma Sintering (SPS) method. Si_3N_4, Al_2O_3, AlN and TiO_2 powders were used as precursors. Starting powders were mixed with high energy ball milling and then were sintered by SPS method (at 1750 °C under pressure of 30 MPa for 12 min.). The milled powders had an average particle size of below ~ 155 nm. The XRD patterns of SPS-ed composites showed that the entire β-SiAlON phase constituent was in the form of $Si_4Al_2O_2N_6$ phase and cubic TiN phase can be formed by the phase transformation of TiO2 in relation with other precursors. FESEM micrographs confirmed that TiN particles were distributed homogeneously throughout β-SiAlON matrix. Mechanical properties evaluation revealed that by adding micro sized TiO_2, optimal mechanical properties with a hardness ~ 14.6 GPa and a fracture toughness ~ 6.3 MPa $m^{1/2}$ were obtained. The improvement in the fracture toughness was attributed to the presence of the crack deflection as the dominant toughening mechanism in the SPS-ed β–SiAlON/TiN composites.

1. Introduction

Ceramics of silicon nitride are one of the most widely used engineering materials due to their high strength, good friction and oxidation properties, low density and high erosion and chemical corrosion resistance [1]. By substitution of silicon nitrogen bond for aluminum oxygen one in beta silicon nitride a solid solution is made which called primarily beta prime silicon nitride, beta prime SiAlON and nowadays beta SiAlON [1–3]. They were discovered in 1970 and actively developed [2,4,5]. The most marvelous structure of SiAlON is β-SiAlON ($Si_{6-z}Al_zO_zN_{8-z}$), where z varies from 0 (pure Si_3N_4) to 4.2 with a structure similar to hexagonal β-Si_3N_4 [6–8]. Other forms of SiAlON are α, O and X-SiAlON [7].

Many efforts have been done to improve ceramics properties via well definable composition and microstructure by carefully controlling the process parameters and methods [8–10]. Similar to almost all the ceramic materials, however, low resistance to fracture has limited the application of silicon nitride based ceramics. The fracture toughness of hot-pressed Si_3N_4 is typically 3–5 MPa $m^{1/2}$ [11]. The problem of the low fracture toughness of the ceramic materials can be overcome by designing composite materials reinforced with a suitable second component [12]. The addition of particulate TiN as a reinforcement can enhance the fracture toughness of the SiAlON materials [13–15]. β-SiAlON/TiN composites are widely attracted the attention of many researchers due to their good thermal shock and corrosion resistance, enhanced mechanical properties, thermal and dimensional stability [15–21].

SiAlON/TiN nanocomposites can be synthesized by planetary ball milling of different compositions of powders like Si_3N_4, TiN, Ti, Al_2o_3 and AlN [7,18,22–24]. Available sintering techniques of SiAlON and its nanocomposites via solid state routes range from gas pressure sintering to pressure less sintering [4]. Introduction of liquid phases into the SiAlON composite system during sintering is one of the most important progresses to obtain ceramics with high performances [20]. Usually, metals and rare earth metal oxides (e.g Al_2O_3, TiO_2 and Y_2O_3) are used as sintering additives which promote densification through the liquid phase sintering [16,17,22,25]. By using Si_3N_4, Al_2O_3, TiO_2 and AlN as starting materials, the first three materials reacts to each other and as a result a low-viscosity liquid phase with low SiO_2 content forms, thereby grain boundary glasses develops [26,27].

Spark plasma sintering (SPS) is a novel sintering technique that allows sintering of hard-to-sinter materials to full density very rapidity [21,22,28]. Compared to conventional sintering (CS) techniques such as pressureless sintering (PLS), hot pressing (HP) or hot iso static pressing (HIP), SPS provides much faster heating rates, shorter sintering times in the range of some minutes [29–31]. Also, with commonly lower sintering temperatures, getting total densification with negligible grain growth and/or phase transformation allowed [32–34]. There have been several studies dealing with the sintering of silicon nitride-based ceramics using SPS technique [20,34]. By utilizing Si_3N_4 and TiN nano-powder as the starting materials, Si_3N_4/TiN nanocomposites with full density have been fabricated successfully via SPS technique and the nanocomposite containing 10 wt% TiN had the highest toughness of ~ 4.9 MPa $m^{1/2}$ [15]. Nevertheless, C. Tian et al. [35] have made Si_3N_4/TiN nanocomposites containing 10 wt.% TiN with toughness of ~ 6.7 MPa $m^{1/2}$ by HP and

* Corresponding author.
Email address: rakhosroshahi@Gmail.com (R.A. Khosroshahi)

http://dx.doi.org/10.1016/j.ijrmhm.2016.08.002
0263-4368/

H. Mandal et al. [18] have received β - SiAlON with toughness of ~ 5.6 MPa $m^{1/2}$ by GPS.

The PLS of β-SiAlON from low cost combustion synthesized Si_3N_4 powders has been previously studied by H. Mandal et al. [18], but they didn't report SPS of SiAlON and its composites with TiN. There for; the objective of this study was to develop SiAlON/TiN composites, with good mechanical properties and low sintering temperature by incorporating low cost combustion synthesized β-Si_3N_4 and TiO_2 powders. In the present work, SiAlON/TiN ceramics were prepared using the SPS sintering process. Phase composition, densification, microstructure and mechanical properties of the bulk samples were investigated.

2. Exprimental procedure

Specimens were prepared from high-purity (˃99 wt%) powders with composition by weight percent according to Table 1. Si_3N_4 (β-Si_3N_4 composition, − 325 mesh powder size), AlN (powder size: < 10 μm), two batch of TiO_2 (powder size: Nanometer powder and submicron powder) and Al_2O_3 (powder size: < 50 nm) were selected as starting materials for synthesizing SiAlON/TiN nanocomposites. Si_3N_4 powders were purchased from Beijing Chanlian-Dacheng Trade Co., China and other powders were bought from Sigma-Aldrich.

The mixture of starting materials was milled in isopropanol alcohol for 10 h in a poly amid jar using Al_2O_3 balls by planetary ball mill (PM2400, 400 rpm). The ball-to-powder weight ratio of 10:1 was used. The obtained slurry was dried and sieved to prepare fine and uniform powder mixtures for spark plasma sintering. Spark plasma sintering was conducted in vacuum at 1750 °C for 12 min. The heating rate was set at 30 °C/min and an applied pressure of 30 MPa was used. Graphite foils were used to constraint and prevent sticking of powders to die during spark plasma sintering. An optical pyrometer that placed on a hole on the surface of the carbon die was used for monitoring temperature during sintering. The set-up (Nanozint 10) allowed cooling rate of ˃200 °C/min in the temperature range up to 100 °C/min.

The powders were suspended in distilled water and then ultrasonically treated and then the particle size distribution of the milled powder was measured by a laser interferometer (Horiba, LB-550). The density of the samples was measured by the Archimedes method in distilled water as an immersing medium. For determining phase composition of the samples, x-ray diffraction patterns (X'Pert. P W 3040/60 philips, CuK_α radiation) in the range of 10–90° (2θ) were collected.

The SPS set-up enabled us to draw the temperature and shrinkage changes according to the sintering time. For microstructure study of the samples by FESEM (SEM: MIRA, TESCAN) and energy-dispersive X-ray spectroscopy (EDS), all samples were polished using 300 up to 1500 SiC grit and standard diamond polishing techniques. Density of specimens was carefully measured by archimedes method. The micrographs were recorded in back scattered electron mode (BSE). Vickers hardness of the samples was measured by applying a load of 10 kg (HV 10) for 15 s (Instron Wolpert, MX-96604) [36]. Toughness measurements carried out by measuring the dimensions of indenture crack effect (by SEM secondary electron mode or optical microscopy) using Anstis and Nihara method [6,16,37].

Table 1
Composition of different SiAlON/TiN composite.

Sample	S_3N_4	Al_2O_3	AlN	TiO_2	Predicted TiN
SB	Rest	15.56	9.33	0	0
SBM	Rest	15.56	9.33	15 (micronized)	13
SBN	Rest	15.56	9.33	15 (micronized)	13

3. Results and discussion

Measuring of particle sizes by laser interferometer characterized the average particle size of the SB, SBM and SBN powders after 10 h mechanical alloying, about 120, 155 and 98 nm respectively.

High energy ball milling was successfully used to mix starting precursors homogenously and the particle size of the mixed powder was reduced. Fig. 1 showed the FESEM image of the SB, SBM and SBN powders composition after high energy ball milling. It was obvious that after grinding the obtained powders with very small particle size of the average values below 150 nm could be gained.

Fig. 2 showed x-ray diffraction patterns of samples SB, SBM and SBN spark plasma sintered (from 10 h milled powders) at 1750 °C. The rapid crystallization of amorphous phases in milled powders has occurred. XRD analysis revealed that SB, SBM and SBN were poly-phase materials consisting the main phase of β-SiAlON. The maxima XRD peaks of β-Si_3N_4 was shifted towards the left hand that confirmed the existence of β-SiAlON in product [19]. Also, the overall composition of β-SiAlON phase in sintered samples was $Si_4Al_2O_2N_6$ (Z = 2) with some X-SiAlON and O-SiAlON. Results showed that TiN phase was in the X-ray patterns with major phases in SBM and SBN samples. Existence of β-SiAlON at 1750 °C sintered sample was due to the mechano chemically activation of the fine powder which had good tendency to be converted to β-SiAlON phase. This may also be attributed to this fact that by modifying sintering temperature, unchanged β-Si_3N_4 phase was not found in the specimens [23,38–40]. The minor obtained phases like X-SiAlON ($Si_3Al_6O_{12}N_2$) and O-SiAlON ($Si_6Al_{10}O_{21}N_4$) were metastable phases at higher temperature and would transform to β-SiAlON during the high sintering temperature or post heat treatment [41]. On the other hand, XRD characterization results showed that by SPS process during 72 min (60 min need for receiving sintering temperature + 12 min dwelling time) crystallization have completed. The intensity of TiN peaks had an increase with decreasing of TiO_2 precursor particle size. Additionally, The XRD results of SBM and SBN verified that the excess using of additives like TiO_2 caused remaining of amorphous phases after densification [8]. And, the fast cooling rate of SPS process hindered phases changes like β-Si_3N_4 to α-Si_3N_4 [8].

The mechanism of reaching to β-SiAlON–TiN composite can be written as follows: Due to eventually reactions of silicon nitride with alumina and aluminum nitride, β-SiAlON has formed by increasing the temperature. TiO_2 take parted in reactions for producing of TiN and by reducing the temperature of reaching to SiAlON - TiN compounds. The formation reactions of SiAlON and TiN can be written as Eqs. (1) and (2) [22,26,27,42–48]:

$$(6-z)/3\ Si_3N_4 + z/3\ Al_2O_3 + z/3AlN \rightarrow Si_{6-z}Al_zO_zN_{8-z}\ (0 \le z \le 4.2) \quad (1)$$

$$1/3\ Si_3N_4 + TiO_2 \rightarrow SiO_2 + TiN + 1/6N_2 \quad (2)$$

It has been reported [3] that the Reaction (1) could be occurred under reducing conditions or at temperatures above 1350 °C [49]. Thus keeping sintering temperature sufficiently above this temper-

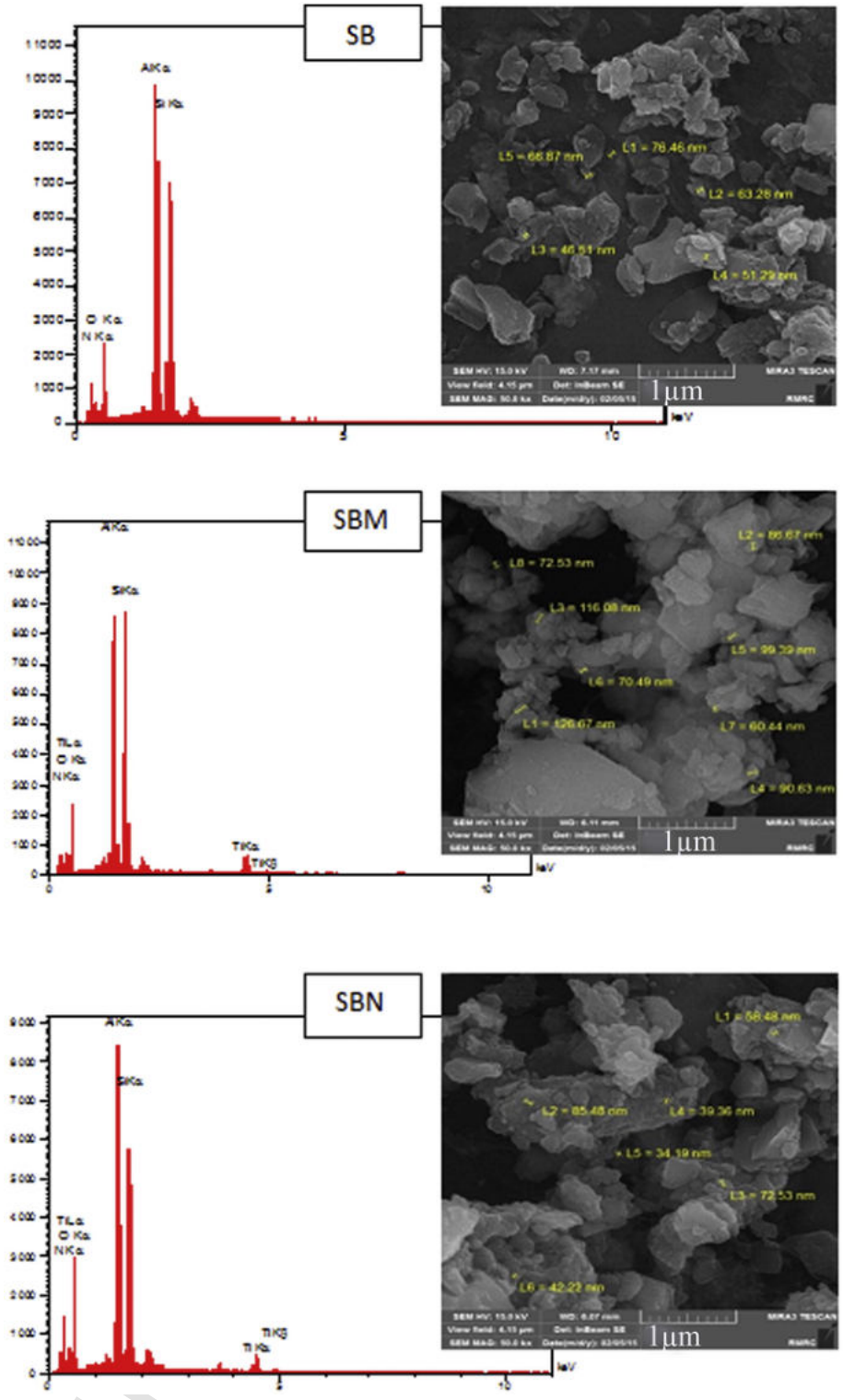

Fig. 1. FESEM images of SB, SBM and SBN powders obtained from high energy ball milling.

ature could be motivated Reaction (1). In the present work, in comparison to conventional sintering techniques by employing SPS technique sintering temperature and time were reduced to 1750 °C and 12 min respectively. Thus, formation of unwanted phases was suppressed during sintering process. Moreover, the successful retaining of transformable phases in the SiAlON matrix would be valuable in improving mechanical properties of the composites [49].

The microstructure of the β-SiAlON/TiN nanocomposites SPS-ed at 1750 °C for 12 min is shown in Fig. 3. The micrographs on the back scattered mode showed that, two areas were well distinguished from the image: light areas represent TiN phase and dark areas

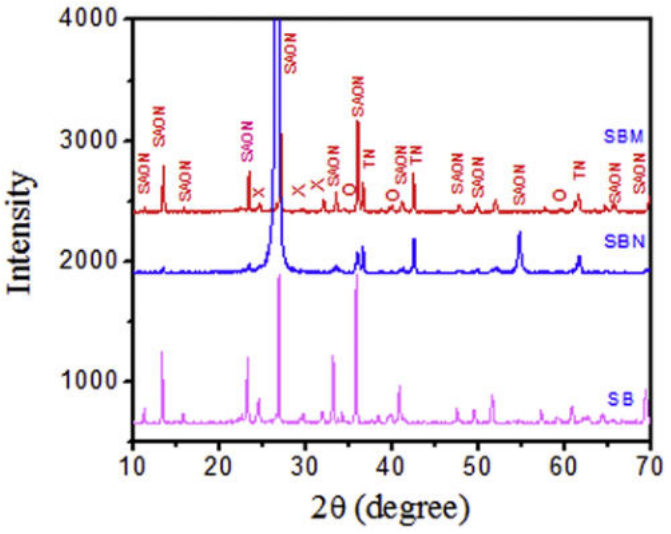

Fig. 2. XRD patterns of the SPS-ed samples at 1750 °C for 12 min. TiN and $Si_4Al_2O_2N_6$ phases have labeled with TN and SAON, respectively. O-SiAlON and X-SiAlON phases have labeled with O and X respectively.

SiAlON. It can be observed that the microstructure was dense with no porosity and TiN particles were distributed homogenously in the SiAlON matrix, which helped full densification of SPS-ed SiAlON/TiN composites [15]. In addition there were some gray areas located beyond the TiN particles and between TiN and SiAlON phases. According to the XRD results (Fig. 2), they could be X-SiAlON or O-SiAlON phase. These phases were products of reactions that occurred in a liquid phase under the presence of the oxide components and β-Si_3N_4 which were dissolved in the liquid during sintering process [11]. This grain boundary phases have seen clearly in SPS-ed materials that were remained after sintering in the samples due to use of Al_2O_3 and AlN as a sintering aid.

On the other hand, in SPS-ed samples large amount of liquid phase and more finer particles of milled samples have prompted particle rearrangement at lower temperature (1750 °C) with a higher shrinkage rate, utilizing full densification [50]. SEM-EDS analyses of SB (point A and point B in Fig. 3) showed that the highest amount of nitrogen (44 At% N, 25 At% O, 20 At% Al and 26 At% Si), which was approximately consistent with the composition of $Si_4Al_2O_2N_6$ in section A, and lowest amount of nitrogen (22 At% N, 42 At% O, 17 At% Al and 18 At% Si), which was approximately consistent with the composition of $Si_6Al_{10}O_{21}N_4$ in section B (grain boundary region), were exist. Due to secondary chemical compositions that were existed with high concentration at grain boundaries, softening of SiAlON at high temperature would be happen [49]. Also, this glassy phases decrease the strength of bulk ceramics like SiAlON, but this phases are need for thermal shock resistance and toughness increment [49].

Fig. 4 showed densification curves of SB, SBM and SBN samples which were spark plasma sintered at 1750 ℃ for 12 min under 30 MPa, which demonstrated the displacement of the upper punch during the process as a function of sintering time. All the samples reached nearly full density by SPS process. The densification curves of SBM and SBN samples (Fig. 4) showed that by addition of TiO_2 component to the initial composition, the onset and the final point of sintering densification occurred at the lower temperatures. The results implied that, the composites (SBM and SBN) shrinkage start point was 1100 °C and 1035 °C, respectively. But the start point for SB sample was 1295 °C. The onset temperature of densification process is lowered to approximately 1035 °C, and the ending temperature of the densification was approximately 1650 ℃ for SBN composition, which were over 260 °C and 50 °C respectively lower than that of SB without TiO_2 component. It can be directly concluded that the addition of TiO_2 into initial powder mixture could decrease sintering temperature. The SiO_2 component was always present as a surface layer on the silicon nitride particles. With increasing oxide content more TiO_2 phase was available for further liquid phase generation and there for the sintering temperature is much more decreased [50].

The specimen densification started at lower temperatures due to being of eutectic temperature of compounds below 1500 °C. Also, construction of liquid phases at this temperature has caused sharp SPS punch displacement. The subsequent sharp displacement or shrinkage at the higher temperature, i.e. 1300–1450 °C can be caused by plastic deformation due to rearrangement mechanism [51]. It can be concluded that the densification of the samples after liquid phase sintering is due to the existence of Al_2O_3, AlN and TiO_2 which is related to the effect of particles rearrangement and/or softening of the amorphous Si-Al-O-N [52].

In the present study, the SiAlON-TiN composites were sintered to full density at reduced time and temperature i.e. 1750 °C and 12 min respectively, comparing to CS techniques. Cain et al. [3] have used HP to sinter similar compositions in the Si_3N_4-TiN system. They found that sintering at 1700 °C was necessary to reach a relative density of 96% for Si_3N_4–10 wt% composite. According to the Fig. 4, however, sample with similar composition could be receive to full density at just 1595 °C by SPS. The existence of electromechanical forces acting over the liquid phase which was formed during sintering

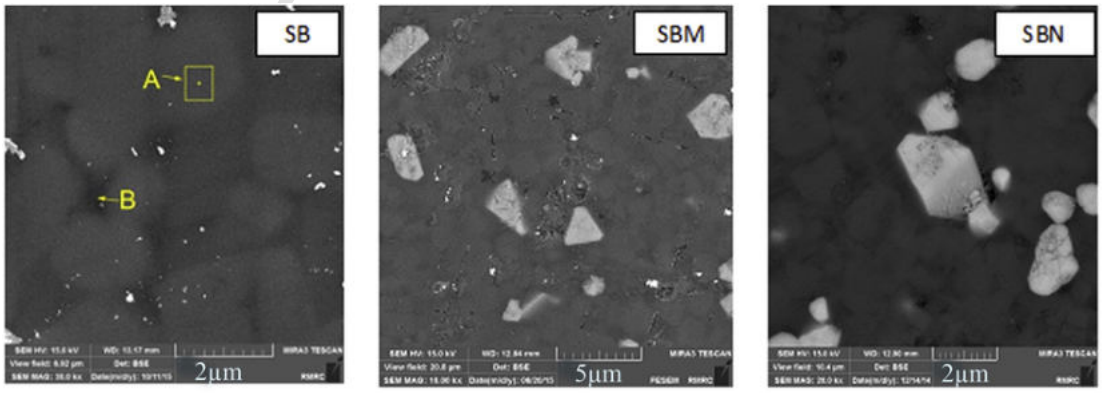

Fig. 3. Microstructure of SB, SBM and SBN samples SPS-ed at 1750 °C for 12 min.

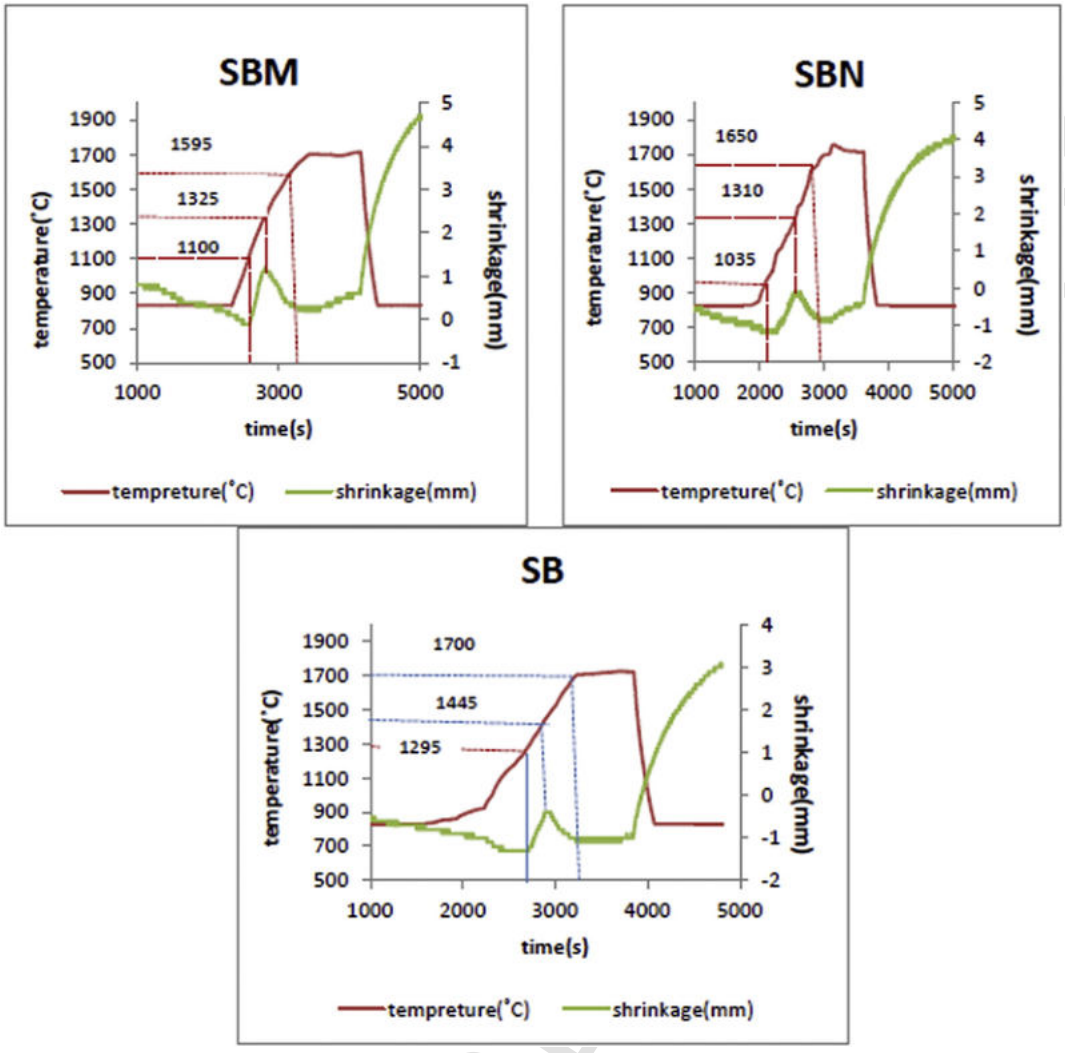

Fig. 4. The densification curves for SB, SBM and SBN composites SPS-ed at 1750 °C for 12 min.

would be a plausible explanation of the reduced sintering temperature and time in SPS-ed Si_3N_4 based composites [5]. Furthermore, the use of nano-sized powder with a high specific surface area for preparing the samples promoted densification process due to the increment in grain boundary diffusion [10].

Fig. 5 showed the dependence of the hardness and fracture toughness of the SPS-ed composites. There can be seen that hardness increased from ~ 14.1 to ~ 15.7 GPa with the decrement of TiO_2 particle size from micron to nanosize. It is well known that the hardness values in the multiphase samples are affected by the intrinsic hardness of constituents. The hardness values increased with the decrease of TiO_2 particle size due to the lower hardness of SiAlON comparing to its composites. H. Mandal [18] and C. Tian [35] were reported hardness values of SiAlON and SiAlON - TiN ceramics between ~ 13 GPa and ~ 15.6 GPa respectively [18]. The fracture toughness increased with the increase of TiO2 particle size. Sample without TiO_2 additive had a fracture toughness of ~ 4.8 MP $m^{1/2}$, while with the addition of 15 wt% TiO_2, fracture toughness increased about 31% to ~ 6.3 MPa $m^{1/2}$. From the FESEM results it was obvious (Fig. 6) that with the increase of TiO_2 particle size in the initial chemical composition increment in the Toughness corresponding to the increase of cracks path in the samples with higher TiO_2 particle size

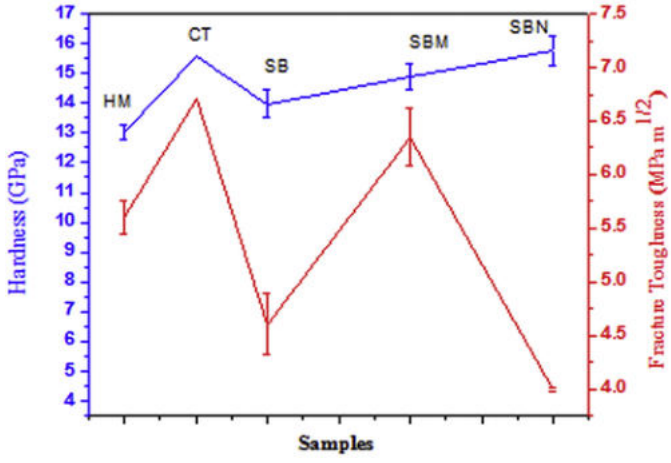

Fig. 5. The dependence of hardness and fracture toughness values of the SPS-ed composites to the samples. H. Mandal results labeled with HM and C. Tian results labeled with CT.

has occurred. This scenario showed this means that the cracks path increment could be the dominant mechanism responsible for tough-

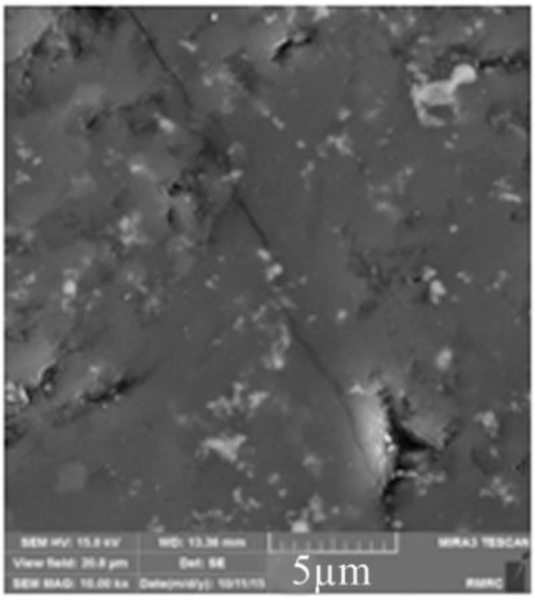

Fig. 6. FESEM photograph of SPS-ed SBM composite after toughness measurement.

ening in the SPS-ed SiAlON-TiN composites which were studied in the present work. SBM showed good hardness and fracture toughness of ~ 14.6 GPa and ~ 6.3 MPa $m^{1/2}$ respectively. Also, due to large particle sizes of TiN in SBM the toughness have been increased [53]. As clearly seen, the nanocomposite processed with benefits high fracture toughness in expense of a little reduction in hardness. It implies that the main aim of the present research is attained. Also, due to secondary chemical compositions, that exist with high concentration at grain boundaries, softening of SiAlON at high temperature would happen [49]. Also, this glassy phases decreased the strength of bulk ceramics like SiAlON, but this phases were need for thermal shock resistance and toughness increment [49]. The studies about active toughening mechanisms in SPS-ed nanocomposites were underway and their results would be publish in forthcoming future. But, based on FESEM results crack deflection was the first suggestion.

4. Conclusions

In this work, the TiN toughened beta SiAlON nanocomposite ceramics were obtained successfully, via low cost Si_3N_4 and TiO_2 powder by combination of mechanical alloying and SPS method. Also by improving and using this technique results regarding the PLS-ed samples, possible mass production of β-SiAlON/TiN were expected. From the experimental results and the above – stated discussion the following results were concluded:

1. After milling for 10 h, a homogeneous nanopowder with length - scale down to 150 nm were produced. Also, Mechanical activation of the precursors reduced the temperature associated with the formation of the liquid phase and furthermore it improved the densification.
2. The addition of TiO_2 as a source of TiN, decreased the sintering temperature from 1700 to 1595 °C by improving liquid phase sintering. Also, it is shown that cubic TiN phase can be formed by phase transformation of TiO_2 in relation with other precursors.
3. It was observed that, spark plasma sintering of the β-SiAlON/TiN powder at temperatures as low as 1750 °C resulted to full density ceramics.
4. β-SiAlON/TiN SPS Sintered samples from micronized TiO_2 showed good hardness and fracture toughness of ~ 14.6 GPa and ~ 6.3 MPa $m^{1/2}$ respectively. It implies that the main aim of the present research is attained.
5. The major reason for improving the fracture toughness would be crack deflection.

References

[1] H.P. Peng, "Spark Plasma Sintering of Si3N4-Based Ceramics: -Sintering Mechanism-Tailoring Microstructure-Evaluating Properties-," Doctor of Philosophy, Intellecta DocuSys, Stockholm, S-10691 Stockholm Sweden, 2004.
[2] X. Yi, T. Akiyama, K. Kurokawa, Combustion synthesis and spark plasma sintering of b-SiAlON, in: A.A. Gromov, L.N. Chukhlomina (Eds.), Nitride Ceramics: Combustion Synthesis, Properties, and Applications vol. 1, Wiley-VCH Verlag GmbH & Co., Germany ed. KGaA, Boschstr. 12, 69469 Weinheim, Germany, 2015, p. 358.
[3] N.G. Ramadan, "Rare-earth Doped (alpha/beta)-siAlON," Doctor of Philosophy, Department of Physics Centre for Advanced Materials, University of Warwick, institutional repository, 2001.
[4] S. Kurama, The effects of processing on the α ↔ β SiAlON transformation during cycling heat treatments, Mater. Sci. Eng. A 487 (2008) 278–288.
[5] A. Kheirandish, K.A. Nekouee, R. Khosroshahi, N. Ehsani, Self-propagating high temperature synthesis of SiAlON, Int. J. Refract. Met. Hard Mater. 55 (2016) 68–79.
[6] P. Pettersson, Z. Shen, M. Johnsson, M. Nygren, Thermal shock resistance of α/β-sialon ceramic composites, J. Eur. Ceram. Soc. 21 (2001) 999–1005.
[7] K.J. MacKenzie, J. Temuujin, M.E. Smith, K. Okada, Y. Kameshima, Mechanochemical processing of sialon compositions, J. Eur. Ceram. Soc. 23 (2003) 1069–1082.
[8] S. Kurama, I. Schulz, M. Herrmann, Wear properties of α-and α/β-SiAlON ceramics obtained by gas pressure sintering and spark plasma sintering, J. Eur. Ceram. Soc. 31 (2011) 921–930.
[9] M.I. Jones, K. Hirao, H. Hyuga, Y. Yamauchi, S. Kanzaki, Wear properties of Y–α/β composite sialon ceramics, J. Eur. Ceram. Soc. 23 (2003) 1743–1750.
[10] B. Nayebi, M.S. Asl, M.G. Kakroudi, M. Shokouhimehr, Temperature dependence of microstructure evolution during hot pressing of ZrB_2–30 vol.% SiC composites, Int. J. Refract. Met. Hard Mater. 54 (2016) 7–13.
[11] F. Lange, L. Falk, B. Davis, Structural ceramics based on Si 3 N 4–ZrO 2 (+ Y 2 O 3) compositions, J. Mater. Res. 2 (1987) 66–76.
[12] A.S. Namini, S.N.S. Gogani, M.S. Asl, K. Farhadi, M.G. Kakroudi, A. Mohammadzadeh, Microstructural development and mechanical properties of hot pressed SiC reinforced TiB 2 based composite, Int. J. Refract. Met. Hard Mater. 51 (2015) 169–179.
[13] T. Ekström, M. Nygren, SiAION ceramics, J. Am. Ceram. Soc. 75 (1992) 259–276.
[14] M. Mitomo, Y. Tajima, Sintering, properties and applications of silicon nitride and sialon ceramics, Nippon seramikkusu kyokai gakujutsu ronbunshi 99 (1991) 1014–1025.
[15] C.H. Lee, H.H. Lu, C.A. Wang, P.K. Nayak, J.L. Huang, Microstructure and mechanical properties of TiN/Si_3N_4 nanocomposites by spark plasma sintering (SPS), J. Alloys Compd. 508 (2010) 540–545.
[16] O. Eser, S. Kurama, The effect of the wet-milling process on sintering temperature and the amount of additive of SiAlON ceramics, Ceram. Int. 36 (2010) 1283–1288.
[17] M. Herrmann, S. Höhn, A. Bales, Kinetics of rare earth incorporation and its role in densification and microstructure formation of α-siAlON, J. Eur. Ceram. Soc. 32 (2012) 1313–1319.
[18] H. Mandal, N.C. Acikbas, Processing, characterization and mechanical properties of SiAlONs produced from low cost β-Si_3N_4 powder, Kona Powder Part. J. 30 (2013) 22–30.
[19] I. Zalite, N. Zilinska, I. Steins, J. Krastins, Spark plasma sintering of SiAlON nanopowders, In: IOP Conference Series: Materials Science and Engineering, 2011, p. 012022.
[20] P. Miranzo, J. González-Julián, M.I. Osendi, M. Belmonte, Enhanced particle rearrangement during liquid phase spark plasma sintering of silicon nitride-based ceramics, Ceram. Int. 37 (2011) 159–166.
[21] X. Yi, K. Watanabe, T. Akiyama, Fabrication of dense β-SiAlON by a combination of combustion synthesis (CS) and spark plasma sintering (SPS), Intermetallics 18 (2010) 536–541.
[22] N. Ahmad, H. Sueyoshi, Properties of Si_3N_4–TiN composites fabricated by spark plasma sintering by using a mixture of Si_3N_4 and Ti powders, Ceram. Int. 36 (2010) 491–496.

[23] O. Eser, S. Kurama, A comparison of sintering techniques using different particle sized β-SiAlON powders, J. Eur. Ceram. Soc. 32 (2012) 1343–1347.
[24] M. Sopicka-Lizer, M. Tańcula, T. Włodek, K. Rodak, M. Hüller, V. Kochnev, et al., The effect of mechanical activation on the properties of β-sialon precursors, J. Eur. Ceram. Soc. 28 (2008) 279–288.
[25] J. Souza, C. Santos, C. Kelly, O. Silva, Development of α-SiAlON-SiC ceramic composites by liquid phase sintering, Int. J. Refract. Met. Hard Mater. 25 (2007) 77–81.
[26] T.G. Tien, Use of Phase Diagrams in the Study of Silicon Nitride Ceramics, Department of Materials Science and Engineering, vol. University of Michigan, 1995.
[27] K. Krnel, A. Maglica, T. Kosmač, β-SiAlON/TiN nanocomposites prepared from TiO 2-coated Si 3 N 4 powder, J. Eur. Ceram. Soc. 28 (2008) 953–957.
[28] M.S. Asl, M.G. Kakroudi, F. Golestani-Fard, H. Nasiri, A Taguchi approach to the influence of hot pressing parameters and SiC content on the sinterability of ZrB_2-based composites, Int. J. Refract. Met. Hard Mater. 51 (2015) 81–90.
[29] R. Orru, R. Licheri, A.M. Locci, A. Cincotti, G. Cao, Consolidation/synthesis of materials by electric current activated/assisted sintering, Mater. Sci. Eng. R. Rep. 63 (2009) 127–287.
[30] M.S. Asl, M.G. Kakroudi, M. Rezvani, F. Golestani-Fard, Significance of hot pressing parameters on the microstructure and densification behavior of zirconium diboride, Int. J. Refract. Met. Hard Mater. 50 (2015) 140–145.
[31] N.P. Vafa, B. Nayebi, M.S. Asl, M.J. Zamharir, M.G. Kakroudi, Reactive hot pressing of ZrB_2-based composites with changes in ZrO 2/SiC ratio and sintering conditions. Part II: mechanical behavior, Ceram. Int. 42 (2016) 2724–2733.
[32] M.I. Jones, K. Hirao, H. Hyuga, Y. Yamauchi, Z. Shen, M. Nygren, Wear properties of self-reinforced α-SiAlON ceramics produced by spark plasma sintering, Wear 257 (2004) 292–296.
[33] F. Ye, Z. Hou, H. Zhang, L. Liu, Y. Zhou, Spark plasma sintering of cBN/β-SiAlON composites, Mater. Sci. Eng. A 527 (2010) 4723–4726.
[34] M. Belmonte, J. González-Julián, P. Miranzo, M. Osendi, Spark plasma sintering: a powerful tool to develop new silicon nitride-based materials, J. Eur. Ceram. Soc. 30 (2010) 2937–2946.
[35] C. Tian, H. Jiang, N. Liu, Thermal shock behavior of Si_3N_4–TiN nano-composites, Int. J. Refract. Met. Hard Mater. 29 (2011) 14–20.
[36] C. Ullner, A. Germak, H. Le Doussal, R. Morrell, T. Reich, W. Vandermeulen, Hardness testing on advanced technical ceramics, J. Eur. Ceram. Soc. 21 (2001) 439–451.
[37] G. Anstis, P. Chantikul, B.R. Lawn, D. Marshall, A critical evaluation of indentation techniques for measuring fracture toughness: I, direct crack measurements, J. Am. Ceram. Soc. 64 (1981) 533–538.
[38] I. Zalite, N. Zilinska, G. Kladler, SiAlON ceramics from nanopowders, J. Eur. Ceram. Soc. 28 (2008) 901–905.
[39] A. Rosenflanz, I. Chen, Kinetics of phase transformations in SiAlON ceramics: II. Reaction paths, J. Eur. Ceram. Soc. 19 (1999) 2337–2348.
[40] N.C. Acikbas, R. Kumar, F. Kara, H. Mandal, B. Basu, Influence of β- Si_3N_4 particle size and heat treatment on microstructural evolution of α: β-SiAlON ceramics, J. Eur. Ceram. Soc. 31 (2011) 629–635.
[41] H. Mandal, D. Thompson, New heat treatment methods for glass removal from silicon nitride and sialon ceramics, J. Mater. Sci. 35 (2000) 6285–6292.
[42] Y.F. Kargin, S. Ivicheva, A. Lysenkov, N. Ovsyannikov, L. Shvorneva, K. Solntsev, Si_3N_4/TiN composites produced from TiO2-modified Si3N4 powders, Inorg. Mater. 48 (2012) 897–902.
[43] R.G. Duan, G. Roebben, J. Vleugels, O. Van der Biest, In situ formation of Si_2N_2O and TiN in Si_3N_4-based ceramic composites, Acta Mater. 53 (2005) 2547–2554.
[44] M. Herrmann, B. Balzer, C. Schubert, W. Hermel, Densification, microstructure and properties of Si_3N_4 Ti (C, N) composites, J. Eur. Ceram. Soc. 12 (1993) 287–296.
[45] M.B. Trigg, K.H. Jack, The fabrication of O'-siAlON ceramics by pressureless sintering, J. Mater. Sci. 23 (1988) 481–487.
[46] A. Vučković, S. Bošković, B. Matović, M. Vlajic, V. Krstic, Effect of β- Si_3N_4 seeds on densification and fracture toughness of silicon nitride, Ceram. Int. 32 (2006) 303–307.
[47] P. Calloch, New Reaction Paths for Advanced SiAlON/TiN Composites, Doctor of Philosophy in Chemistry, Victoria University of Wellington, Victoria University of Wellington, 2015.
[48] A. Roine, HSC, In: HSC Chemistry 6.0, 6 ed., Outokumpu Research Oy, 2006.
[49] D. Richerson, D.W. Richerson, W.E. Lee, Modern Ceramic Engineering: Properties, Processing, and Use in design, CRC Press, 2005.
[50] X. Xu, T. Nishimura, N. Hirosaki, R.J. Xie, H. Tanaka, Fabrication of a nano-Si_3N_4/Nano-C composite by high-energy ball milling and spark plasma sintering, J. Am. Ceram. Soc. 90 (2007) 1058–1062.
[51] L. Liu, F. Ye, Y. Zhou, Z. Zhang, Q. Hou, Fast bonding α-SiAlON ceramics by spark plasma sintering, J. Eur. Ceram. Soc. 30 (2010) 2683–2689.
[52] M. Sopicka-Lizer, C. Duran, H. Gocmez, T. Pawlik, M. Mikuskiewicz, K. MacKenzie, Effect of high energy milling on the formation and properties of sialon ceramics prepared from silicon nitride-aluminium nitride precursors, Ceram. Int. 39 (2013) 4269–4279.
[53] B. Zou, C. Huang, H. Liu, M. Chen, Preparation and characterization of Si_3N_4/TiN nanocomposites ceramic tool materials, J. Mater. Process. Technol. 209 (2009) 4595–4600.